LEGIBILITY NOTICE

A major purpose of the Technical Information Center is to provide the broadest possible dissemination of information contained in DOE's Research and Development Reports to business, industry, the academic community, and federal, state, and local governments. Non-DOE originated information is also disseminated by the Technical Information Center to support ongoing DOE programs.

Although large portions of this report are not reproducible, it is being made available only in paper copy form to facilitate the availability of those parts of the document which are legible. Copies may be obtained from the National Technical Information Service. Authorized recipients may obtain a copy directly from the Department of Energy's Technical Information Center.

LA-UR 90-2092

Los Alamos National Laboratory is operated by the University of California for the United States Department of Energy under contract W-7405-ENG-36

LA-UR--90-2092

DE90 013161

TITLE INTERNAL DYNAMICS OF ELECTRICAL DISCHARGES

AUTHOR(S) A. Kadish, William B. Maier II
Atmospheric Sciences Group
Los Alamos National Laboratory, Los Alamos, NM

K. T. Robiscoe
Montana State University
Bozeman, MT

SUBMITTED TO XIVth INTERNATIONAL SYMPOSIUM ON DISHCARGES
AND ELECTRICAL INSULATION IN VACUUM
Santa Fe, NM
September 17-20, 1990

DISCLAIMER

Los Alamos Los Alamos National Laboratory
Los Alamos, New Mexico 87545

INTERNAL DYNAMICS OF ELECTRICAL DISCHARGES

A. Kadish, William B. Maier II
Los Alamos National Laboratory
Los Alamos, NM 87545

R. T. Robiscoe
Montana State University
Bozeman, MT 59717

Abstract

The existence of thresholds for electrical discharge onset suggests a functional relation between macroscopic resistivity and current. At low current, the resistivity should be inversely proportional to the magnitude of the current. Macroscopic models which employ this scaling predict many empirically observed properties of transient electrical discharges, such as *(i)* thresholds for onset of current, *(ii)* abrupt termination of current in active regions of a current channel, *(iii)* current restart in passive regions of current channels, *(iv)* leaders, and *(v)* residual charge, both in channels and at sources when current terminates. We present an overview of research with these models and use examples to illustrate the results that have been obtained. We also show how these models predict current channel formation and describe results of efforts to benchmark theory with experimental data.

I. Introduction

An understanding of internal spatial dynamics is central to predicting and interpreting macroscopic phenomena associated with electrical discharges. For example, far-field electromagnetic radiation from discharges may be expressed as an integral of the retarded time derivative of the macroscopic current density. The integral is over the entire discharge current channel and depends, consequently, on details of the spatial variation of the evolving current density.

Very accurate numerical simulations based on evolving particle trajectories make it possible to study many aspects of electrical discharges in great detail. However, even with the availability and clever utilization of existing mainframes, time stepping requirements render these simulation studies impractical for predicting discharge behavior on time scales comparable to the life of a discharge.

Macroscopic models, on the other hand, allow one to study the entire evolution of a discharge, but at a price. The usefulness of a model depends strongly on the physical relevance of the modeling of discharge parameters, as well as on uncertainties in boundary and initial conditions. Some guidance for the model is provided by experiment. Specifically, the voltage drop across many DC discharges tends to depend very weakly on discharge current, *i.e.*, RIII=V*, where V* is a constant.

In addition, any model aspiring to describe an electrical discharge over its entire lifetime must account for several empirical observations. Field and/or voltage thresholds are required for the onset of a discharge current. Discharge current can terminate abruptly with charge remaining at the source and in the current channel.

The existence of thresholds for current onset may be interpreted as evidence of a strong dissipative, or resistive, mechanism being in place at small current. However, the energy needed to overcome this effect must be finite. For a lumped parameter (LCR) approximation of a discharge, this implies an arc resistance which is inversely proportional to the size of the current when the current is small. The coefficient of proportionality may depend on arc and material histories.

It can be shown that this simple scaling produces many observed properties of transient electrical discharges.[1] These include: (*i*) threshold for discharge onset; (*ii*) abrupt termination of current; (*iii*) residual charge in current channels and charge sources at current termination; and (*iv*) a finite numer of current oscillations, the number depending on initial voltage.

The lumped parameter theory has been benchmarked successfully using available data.[2-4] The success with lumped parameter models suggests a modeling of dissipative mechanisms in 1-D, 2-D, and 3-D models of discharges which includes threshold effects locally. At small currents, the dissipation is presumed to be inversely proportional to the magnitude of the current density. We have incorporated this dependence in both stripline models of surface flashover and plasma-based models of punchthrough arcs.

Using a stripline model,[5-7] we have analyzed charge transport in discharges initiated at a charge spot on a dielectric surface. The surface is backed by a conducting substrate which carries an image current that constitutes the return leg of the stripline. A plasma based model has been employed to study the effect of propagating

electromagnetic waves on current channel dynamics.[8] The propagating waves are determined by boundary conditions at current channel extremities.

In this paper, we derive generic properties of electrical discharge models which utilize the inverse relation between resistivity and current at small values of current. In section III, we describe simple transmission line and plasma-based models of discharges in linear current channels and discuss their remarkable richness in discharge phenomena. In section IV, we present the results of efforts to benchmark theory against experimental data. Those efforts have, to date, been limited by available data to LCR models of discharges.

If details of the spatially-dependent theories test favorably against future experimental data, then a high priority should be assigned to an understanding of dissipative processes in electrical discharges at low current.

II. Models for Electrical Discharges

We describe electrical discharges in terms of an electrical current density, $\vec{j}(\vec{x},t)$, and a finite set of other macroscopic variables, $\{v_k(\vec{x},t);\ k = 1,2,\ldots,m\}$. The set might include voltages, charge densities or components of electromagnetic fields. In general, the current density may be a sum of the current densities of different species of charged particles.

It is convenient to introduce the magnitude of the current density, $j(\vec{x},t) \geq 0$, and the vector, $\vec{e}_j(\vec{x},t)$, in the direction of the current density

$$\vec{j}(\vec{x},t) = j(\vec{x},t)\,\vec{e}_j(\vec{x},t) \qquad (1)$$

Note that $\vec{e}_j$ is defined only if $j > 0$, and that if $j > 0$, $\vec{e}_j$ is a unit vector. When $\vec{j}(\vec{x},t) \neq 0$, we take its evolution to be given by an equation of the form

$$\frac{\partial \vec{j}}{\partial t} = \vec{F} - F^* \vec{e}_j \,. \qquad (2)$$

In eq. (2), $\vec{F}$ and F^* may depend on space, $\vec{x}$, and time, t. The dependence may be both explicit and implicit via $\vec{j}$ and $\{v_k\}$ and spatial derivatives of both $\vec{j}$ and elements of

the set $\{v_k\}$. F^* is restricted to be positive. In particular, F^* may depend on $\vec{e}_j$ (*e.g.*, it may be the double inner product of a matrix with the dyad $\vec{e}_j\vec{e}_j$).

Examples of systems containing current density evolutions of this type are given by lumped circuit (LCR) models,[1] transmission line (distributed parameter) models,[3] and charged fluid (plasma) models[8] of transient electrical discharges in which a dissipative mechanism has been taken at weak current to be inversely proportional to the magnitude of the current density. In applications of these models, the current channel is often assumed to be in the direction of the z-axis. Writing $\vec{j} = \hat{j}\vec{e}_z$, eq. (2) becomes, for simple versions of these systems

$$L\frac{\partial \hat{j}(t)}{\partial t} = V(t) - V^* \operatorname{sgn} \hat{j}; \quad \text{(LCR)}, \tag{2a}$$

$$\hat{L}\frac{\partial \hat{j}(z,t)}{\partial t} = -\frac{\partial V(z,t)}{\partial z} - E^* \operatorname{sgn} \hat{j}; \quad \text{(transmission line)}, \tag{2b}$$

$$\frac{\partial \hat{j}(z,t)}{\partial t} = \omega_p^2(z,t)\,[D(z,t) - D^* \operatorname{sgn} \hat{j}]; \quad \text{(plasma)}, \tag{2c}$$

where $\operatorname{sgn} \hat{j} = +1$ if $\hat{j} > 0$ and $\operatorname{sgn} \hat{j} = -1$ if $\hat{j} < 0$. In eq. (2a), V(t) might be the time-varying voltage across a capacitive charge spot on a dielectric surface and L is an inductance.[1] (In this case $\hat{j}$ is the current rather than the current density.) In eq. (2b), V(z,t) is the time- and space-dependent voltage between the current channel and its image in a conducting substrate and $\hat{L}$ is an inductance per unit length. (Again $\hat{j}$ is the current.) In eq. (2c), ω_p^2 is a plasma frequency, and D(z,t) is the z-component of the electric displacement vector.[4] $V^*(z,t)$, $E^*(z,t)$ and $D^*(z,t)$ are obtained from F^* in eq. (2) by taking the scalar product of that equation with $\hat{e}_z$, the unit vector in the z direction. These LCR, transmission line and plasma models have been analyzed to understand and predict macroscopic properties of lightning, surface flashover and "punchthrough" arcs. They predict threshold conditions for the onset of discharge current, the abrupt termination of discharge current, and residual electrical charge both

in current channels and at charge sources when the discharge terminates.[1,4,8]

The threshold condition for current onset is central to the understanding of the macroscopic evolution of arcs. It is easily derived from eq. (2), whose components parallel and perpendicular to $\vec{e}_j$ are given by

$$\frac{\partial j}{\partial t} = F_{\parallel} - F^*; \qquad F_{\parallel} = \vec{F} \cdot \vec{e}_j \ , \tag{3a}$$

$$\left(j \frac{\partial \vec{e}_j}{\partial t} \right) = \vec{F}_{\perp}; \qquad \vec{F}_{\perp} = \vec{F} - (\vec{F} \cdot \vec{e}_j)\, \vec{e}_j \ , \tag{3b}$$

respectively. We show below that if $j(\vec{x}_0,t_0) = 0$, eq. (3a) implies $j(x_0,t)$ cannot become positive (*i.e.*, there can be no current at $\vec{x}_0$) until $|\vec{F}| > F^*$ at $\vec{x} = \vec{x}_0$. Therefore, $F^*(\vec{x}_0,t)$ is a threshold condition on $|\vec{F}(\vec{x}_0,t)|$ for the onset of discharge current, for $t > t_0$, if $j(\vec{x}_0,t_0) = 0$. In particular, from eqs. (2a) - (2c), we see that V^* is a threshold for the charge spot voltage of the LCR model E^* is a local threshold electric field for the voltage gradient of the transmission line model of surface flashovers, and D^* is a local threshold for the electric displacement vector for the plasma model of arcs.

To demonstrate the threshold condition, we observe that if both $j(\vec{x}_0,t_0) = 0$ and $|\vec{F}(\vec{x}_0,t_0)| < F^*$ and, if one attempts to apply eq. (2), then eq. (3a) implies $\frac{\partial j(\vec{x}_0,t_0)}{\partial t} < 0$, which contradicts $j(\vec{x}_0,t_0) \geq 0$.

As a consequence of the threshold condition, if electric current is flowing at $\vec{x} = \vec{x}_0$ and at some time, $t = t_0$, the current takes the value zero when $|\vec{F}(\vec{x}_0,t_0)| < F^*(x_0,t_0)$, the current at $\vec{x} = \vec{x}_0$ terminates abruptly, and cannot restart until some later time, t, when $|\vec{F}(\vec{x}_0,t)| > F^*(\vec{x}_0,t)$. Thus, the discharge current can terminate with charge remaining in both current channels and charge sources.[4-8]

Equation (3b) determines the evolution of current direction. The initial direction of this vector is that of the initial charge transport. If a channel guides the

transport, it is also the initial direction of the channel. It is important to note that this direction is not arbitrary. It is governed by two factors. The first is obviously given by eq. (3a) which requires that at onset $|\vec{F}\cdot\vec{e}_j| > F^*$. The second is due to the fact that when current first starts to flow at any position, the multiplier of the time derivative of the direction of current is zero.

Suppose $\vec{j}(\vec{x},t_0) = 0$ but $j(\vec{x},t) \neq 0$ for $t_1 \leq t < t_2$ when $t_1 > t_0$. From eqs. (3a) and (3b) we have

$$\vec{e}_j(\vec{x},t) = \vec{e}_j(\vec{x},t_1) + \int_{t_1}^{t} \frac{\vec{F}_\perp(\vec{x},t')}{j(\vec{x},t')}\,dt' , \qquad (4a)$$

$$j(\vec{x},t') = \int_{t_0}^{t'} [F_\parallel(\vec{x},t'') - F^*(\vec{x},t'')]\,dt'' , \qquad (4b)$$

Now suppose that $\lim_{t\to t_0+} \vec{e}_j(\vec{x},t)$ exists, so when $t\to t_0+$ current starts at $t = t_0$ with a well-defined direction. Then the integral on the right hand side must converge as $t_1 \to t_0$. From eq. (4b) we see that for $t' \to t_0$, $j(\vec{x},t')$ is less than or equal to a constant times $t' - t_0$. Therefore, for the integral in eq. (4a) to converge as $t_1 \to t_0$ we must have

$$\lim_{t' \to t_0} \vec{F}_\perp(\vec{x},t') = 0 . \qquad (5)$$

This implies that $\vec{e}_j(\vec{x},t_0+)$ and $\vec{F}(\vec{x},t_0)$ are colinear.

$$\vec{e}_j(\vec{x},t_0+) = \pm \frac{\vec{F}(\vec{x},t_0)}{|\vec{F}(\vec{x},t_0)|} . \qquad (6)$$

Since eq. (3a) shows that $F_\parallel > F^*$, $\vec{e}_j$ must be in the same direction as $\vec{F}$. If electromagnetic waves launch the contiguous discharges, field directions compatible with exceeding threshold need not be colinear with the direction of the previously-opened channel segment. The continuation of the channel may appear to abruptly change direction.

The condition of the medium can significantly affect the direction of current channels. As an example,

suppose $\overleftrightarrow{F}^* = \sum_{i=1}^{3} F_i^* \vec{e}_i \vec{e}_i$ where $\vec{e}_i$ is an orthonormal set of unit vectors (*e.g.*, $\vec{e}_1 = \vec{e}_x$, $\vec{e}_2 = \vec{e}_y$ and $\vec{e}_3 = \vec{e}_z$) and $F^* = \overleftrightarrow{F}^* : \vec{e}_j \vec{e}_j$ where $\vec{e}_j = \vec{j}(\vec{x},t)/j(\vec{x},t)$. If $\vec{F}(\vec{x},t) = \sum_{i=1}^{3} F_i \vec{e}_i$, eq. (6) requires that at current onset we must have

$$\vec{e}_j = \frac{\sum_{i=1}^{3} F_i \vec{e}_i}{\sqrt{\sum_{i=1}^{3} F_i^2}} \tag{7}$$

From eq. (3a) we also must satisfy the threshold condition $F_j - F^* > 0$ which takes the form

$$\sqrt{\sum_{i=1}^{3} F_i^2} \geq \frac{\sum_{i=1}^{3} F_i^* F_i^2}{\sum_{i=1}^{3} F_i^2} . \tag{8}$$

Note that if $F_1^*/|\vec{F}| >> 1$ and $F_2^*/|\vec{F}| >> 1$, the threshold condition becomes $|\vec{F}| > F_3^*$ and $\vec{F} \equiv F_3 \vec{e}_3$ so current flows parallel to $\vec{e}_3$.

III. Spatially-Dependent Discharges

The threshold property implied by our modeling of resistance at low current has profound consequences for charge transport. At the macroscopic level of description, the moving charges which constitute electrical current can be viewed as a fluid. As a result, the evolution of the discharge is governed by wave dynamics of the type commonly encountered in hydrodynamic or magneto-hydrodynamic models. Roughly speaking, the waves which affect the current evolution are of two types: self-consistent, or self-generated waves; and freely-propagating, or externally-generated waves. The effects of these waves on the current are illustrated by two examples, using one-dimensional transmission line and plasma models of discharges.

Figure 1 shows the arc transmission line model we shall analyze. Physically, the arc can originate from a highly-charged spot deposited on a dielectric surface overlying a metal substrate. When the relative spot potential exceeds the surface dielectric breakdown threshold, a transient electrical discharge may occur across the surface. We assume that this discharge, or surface flashover arc, carries current, I, over a length, l, for a short time. Schematically, the flashover arc can be viewed as a transmission line problem, with a generator (charged spot) that supplies a short, strong voltage pulse to a stripline of length, l. The stripline has *distributed* circuit elements: $\hat{R}$ (resistance), $\hat{L}$ (inductance), $\hat{C}$ (capacitance), and $\hat{G}$ (dielectric conductance), all per unit length, and it may be terminated in a load impedance Z_L. The actual arc current, I(x,t), flows in the top leg of the stripline. The charge per unit length on the stripline, $\hat{Q}$, is related to the potential and the capacitance per unit length by $\hat{Q} = \hat{C}V$. The return current in the bottom leg is the image current flowing in the metal substrate. A reasonable choice for the generator is an initially charged capacitor of total capacitance, C_g, with C_g determined by the dielectric thickness and the area of the charge spot. Also, if the arc terminates on a metallic boundary, it is reasonable to set the terminator impedance $Z_L = 0$, which represents a short circuit.

A. FLASHOVER ARC CONFIGURATION

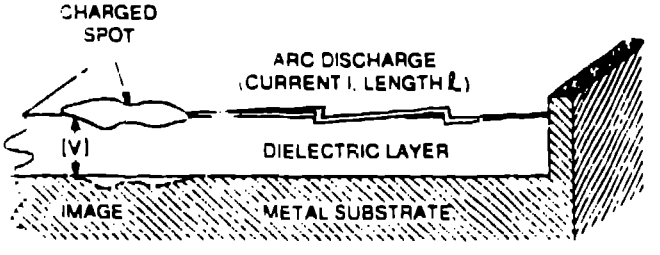

B. ARC STRIPLINE MODEL

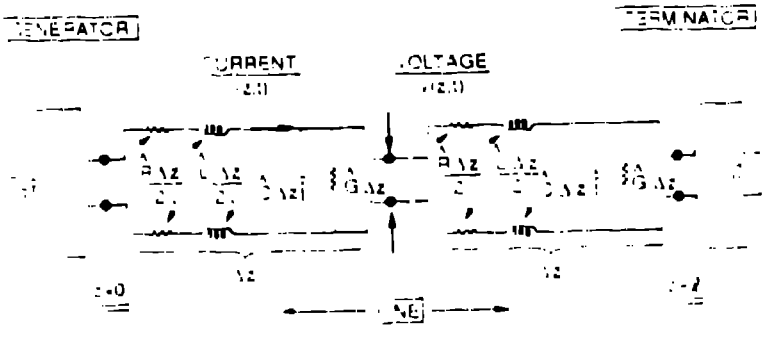

FIG. 1. *(a)* Schematic of a surface flashover. In our model, the charge spot and its image are the capacitor. The arc discharge current and its image are the transmission line. *(b)* The transmission (or stripline) model of the configuration in *(a)*. Differential elements of the discharge and its image are modeled as differential capacitances, inductances, and resistances. The voltage across the differential capacitance is V. The current is I. The charge per unit length on the line is $\hat{C}V$.

If the radiation losses are negligible, the current equations governing the propagation of the current and voltage pulses along the stripline of Fig. 1 are[5]

$$[\hat{R} + \hat{L}\,(\frac{\partial}{\partial t})]\, I = -\frac{\partial V}{\partial z} \,. \tag{9}$$

$$[\hat{G} + \hat{C}\,(\frac{\partial}{\partial t})]\, I = -\frac{\partial I}{\partial z} \,. \tag{10}$$

The arc current along the stripline, I, and voltage across the stripline, V, each depend on both time, t, and position, z, along the arc. The boundary conditions are

$$I(0,t) = -C_g \frac{\partial V(0,t)}{\partial t} \,,$$

$$V(l,t) = Z_L\, I(l,t) \,. \tag{11}$$

For simplicity we shall set $Z_L = 0$ (the arc terminates at a short). Also, we put the dielectric conductance $\hat{G} = 0$; this implies that, during the history of the flashover arc, negligible current leaks through the dielectric. The second boundary condition in eq. (11) becomes $V(l,t) = 0$. Typical initial conditions are those for a charged line:

$$I(z,0) = 0, \quad V(z,0) = V(z). \tag{12}$$

Transmission-line models of electrical discharges employed to date have not been successful in accounting for many of the observed macroscopic properties of arcs. For example, thresholds for discharges, abrupt termination of discharges, and nonzero source voltages at arc termination have not been predicted by such models. We have, for the first time, successfully described these properties of arcs and others by using a lumped circuit model and by imposing an inverse proportionality between arc resistance and current magnitude at low

current.[1] For the stripline model we employ to obtain an understanding of the spatial distribution of charge and current during a discharge, we *postulate* an analogous *local* form of the AWA. Over every infinitesimal interval of length, we require, when $I \neq 0$,

$$\hat{R} = E^*/|I| \ , \tag{13}$$

where E^* is a positive constant. The dimensions of $\hat{R}$ are resistance per unit legnth, so E^* has the dimensions of electric field. Eq. (13) guarantees that the resistive voltage drop per unit length is always $-E^*\mathrm{sgn}I$, where $\mathrm{sgn}I = I/|I|$ for $|I| \neq 0$. Thus, the system is dissipative.

Employing eq. (13) in eqs. (9) and (10) yields, after setting $\hat{G} = 0$,

$$\hat{L}\,\frac{\partial I}{\partial t} + \frac{\partial V}{\partial z} = -E^*\mathrm{sgn}I \ , \tag{14a}$$

$$\hat{C}\,\frac{\partial V}{\partial t} + \frac{\partial I}{\partial z} = 0 \ . \tag{14b}$$

Since the functional dependence of the arc resistance on I has only been specified when $I \neq 0$, eq. (14a) cannot be used without extension to advance I as a function of t when $I(x,t) = 0$ for some non-zero interval of time.

General properties of current and voltage evolution in a surface discharge have been discussed elsewhere.[5] Here we recall that E^* is a threshold which must be exceeded by $|\partial V/\partial x|$ if current is to be initiated. Moreover, in regions of space and time where current flows without changing sign, so $\mathrm{sgn}I$ = constant, differentiation of eqs. (14a) and (14b) yields

$$\left(\frac{\partial^2}{\partial t^2} - \frac{1}{\hat{L}\hat{C}}\,\frac{\partial^2}{\partial z^2}\right)\begin{pmatrix} I \\ V \end{pmatrix} = 0 \ , \tag{15}$$

and I and V satisfy a wave equation with signal speeds $\pm(\hat{L}\,\hat{C})^{-1/2}$. Solutions are determined by initial and boundary data. However, if current flows in an active region of the current channel which abuts a passive region, the boundary between the two is not fixed, but varies in time as voltage gradients which were above or below threshold rise or fall. The motion of this free boundary must be determined as part of the solution to the wave equation. Its motion determines how passive and active regions evolve.

We illustrate some of the arc properties with a simple stripline example.

If the discharge is initiated at a large charge spot at $z = 0$, the voltage at the charge spot, $V(0,t)$, may be taken to be a constant, V_0, over the discharge lifetime. For simplicity, we shall assume the initial active region at $t = 0$ is given by $0 < z < z_1$, with z_1 small, and the initial voltage is given by $V(z,0) = V_0(1-z/z_1)$ for $0 < z \leq z_1$ with $V_0/z_1 > E^*$ and $V(z,0) = 0$ for $z_1 \leq z \leq \ell$. In the limit $z_1 \to 0$, the current front propagates down the stripline with velocity $(\hat{L}\hat{C})^{-1/2}$. Note that at $t = 0$: $-\partial V/\partial z = V_0\delta(z)$. This large voltage gradient, together with the current front dynamics, results in the instantaneous elevation of the current at $z = 0$ to a value $\sqrt{\hat{C}/\hat{L}}\, V_0$. If $V_0 < E^*\ell/2$, the current terminates abruptly everywhere at $t_f = 2\sqrt{\hat{L}\hat{C}}\,(V_0/E^*)$ with the advance of the current front at the position $z_{final} = 2V_0/E^* < \ell$. During discharge at time, $0 < t < t_f$, the current and voltage in the region $0 < z < t\left(\sqrt{\hat{L}\hat{C}}\right)^{-1}$ are given by (see Appendix D of ref. 5)

$$I(z,t) = \frac{E^*}{\hat{L}}\left[\frac{\sqrt{\hat{L}\hat{C}}}{E^*}\, V_0 - \frac{1}{2}\, t\right],$$

$$V(z,t) = V_0 - \frac{1}{2}\, E^* z \,. \qquad (16)$$

Note that when the current vanishes at $t_f = 2\sqrt{\hat{L}\hat{C}}\, V_0/E^*$, $\left|\frac{\partial V}{\partial z}\right| = \frac{1}{2}E^*$, which is below threshold.

For a second example, we assume a cylindrically symmetric current channel of radius, r_0, centered on the z-axis with current restricted to flow in the axial direction: $\hat{e}_j = \pm\, \hat{e}_z$ (see Fig. 2). We use eq. (2c) to describe the current evolution. We take the charge and current densities and the axial electric field to be independent of spatial variation across the channel, and ω_{pi}^2, to facilitate illustration, is taken to be independent of time. In the current channel, the only other non-trivial electromagnetic fields are the radial electric and the azimuthal magnetic field components. These field

components are assumed to be linear in the radial cylindrical polar coordinate. Maxwell's equations and eq. (2c) for the current evolution in active regions of the current channel yield,

$$\frac{\partial \hat{j}}{\partial t} = \omega_p^2 (D - D^* \operatorname{sgn} \hat{j}) \ ,$$

$$\frac{\partial D}{\partial t} + \hat{j} = f\left(t - \frac{z}{c}\right) + g\left(t + \frac{z}{c}\right) \ , \qquad (17)$$

where D is the z-component of the electric displacement, and f and g are electromagnetic waves traveling up and down the current channel with the constant speed of light, c, in the channel. The plasma frequency, ω_p, is presumed constant in time, but may be a function of z.

At t = 0, we assume $\hat{j}(z,0) = 0$ (no initial current) and $|D(z,0)| \le D^*(z)$ (*i.e.*, |D| is below threshold). An intense forward-propagating pulse, $f(t-z/c) = A\delta(t-z/c)$ is introduced at z = 0 with $0 < A < D^*$. We assume g = 0. The propagating pulse arrives at $z > 0$ at time $t_0(z) = z/c$ and instantaneously raises the local value of the axial displacement by an amount, A.

$$D(z,t_0(z)+) = D(z,0) + A = D_0(z) \ . \qquad (18)$$

If $D_0(z) > D^*$, then $\hat{j}(z,t)$ and $D(z,t) - D^*(z)$ execute unforced oscillations on the time interval $t_0(z) < t < t_f(z) = t_0 + \pi/\omega_p(z)$.

$$\hat{j}(z,t) = \omega_p^{-1}(z)\ [D_0(z)-D^*(z)]\ \sin\ [\omega_p(z)(t-t_0(z))] \ ,$$

$$D(z,t) = D^*(z) + [D_0(z)-D^*(z)]\ \cos\ [\omega_p(z)(t-t_0(z))] \ . \qquad (19)$$

When $t = t_f(z)$, we have $\hat{j}(z,t_f(z)) = 0$ and, since $D_0(z) > D^*(z)$ and $A < D^*(z)$, we also have

$$D^*(z) \ge D(z,t_f(z)) = 2D^*(z) - D_0(z) \ge D^*(z) - A > 0 \ . \qquad (20)$$

Therefore, $|D(z,t_f(z))|$ is below threshold, and the discharge terminates.

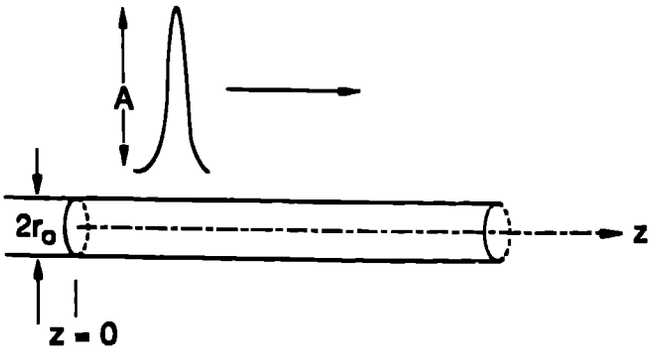

FIG. 2. A steep, narrow, electromagnetic pulse propagates in the positive z-direction along a cylindrically symmetric channel. The pulse raises fields above threshold in some regions of the channel causing discharge current to flow. In other regions, it raises fields to values below those required for the onset of discharge current. Subsequent pulses may raise fields above threshold in these regions.

If a second electromagnetic pulse is now launched at $z = 0$, a process similar to the first occurs with the important difference that current will propagate farther down the current channel. The reason for the advance is that the first pulse has raised the field in the channel even where the current was not driven. In such regions, the passive field is closer to threshold, so the second pulse may make these regions active. In this way, charge is stepped down the channel as a result of successive, freely-propagating, electromagnetic pulses.

IV. Benchmarking the Theory

Even though our models produce features of discharge behavior which qualitatively agree with those exhibited in nature, it is necessary to test the theory by quantitative comparison with empirical data. Some first steps have been taken in this direction. We have compared the simplest possible versions of the theory with Naval Research Laboratory (NRL) data[9] for an underdamped discharge with a 1.7 m current channel and with Texas Tech data[11] for an overdamped arc discharge with length of the order 1 cm.

The NRL discharge was produced by first shining a laser beam along the axis of a gas-filled tank. A Marx bank was then discharged and a gas breakdown discharge was observed in the laser-heated channel. The current amplitude oscillated several times, the number of oscillations depending on the initial Marx bank voltage.

The discharge current was seen to terminate abruptly. The circuit inductance, L = 88 μH, bank capacitance, C = 8 μF, and variable Marx-bank voltage were provided. The external circuit resistance was not measured.

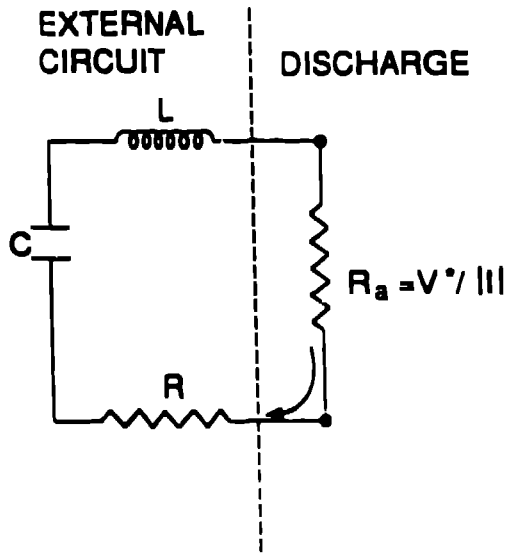

FIG. 3. The LCR circuit used to model electrical discharge experiments at NRL and Texas Tech. When comparing our theory with data, the arc was modeled as resistance with a constant voltage drop $V^* = R|I|$.

In order to test the resistive scaling with current against the NRL data, we modeled their configuration using an LCR circuit (see Fig. 3). Total inductance and capacitance were given the values 88 μH and 8 μF, respectively. The arc was modeled as a resistance equal to a constant, V^*, divided by the magnitude of the current, I. An external resistance, R, was placed in series with the arc (see Fig. 3). The LCR equations are then

$$L\frac{dI}{dt} = V - RI - V^*\mathrm{sgn}I \ ,$$

$$C\frac{dV}{dt} = -I \ , \qquad (2.1)$$

where V is the Marx-bank voltage. We used the data associated with the highest initial Marx-bank voltage to adjust the unknown parameters R and V^*. Using $R = 0.3\Omega$ and $V^* = 1.8$ kV, the theory not only gave the correct number of current oscillations, amplitudes and termination time, but also predicted the surprising shape of the last half-cycle. The fit is shown in Fig. (4). Note the sharp change in the slope of the current at the beginning

of the last half-cycle. From eq. (21), when I = 0, and sgnI changes sign, the derivative of I is discontinuous

$$\left|\delta\left(\frac{dI}{dt}\right)\right| = 2\frac{V^*}{L} . \qquad (22)$$

This discontinuity occurs at all sign changes of the current, but is apparent in the data only when |dI/dt| is smallest.

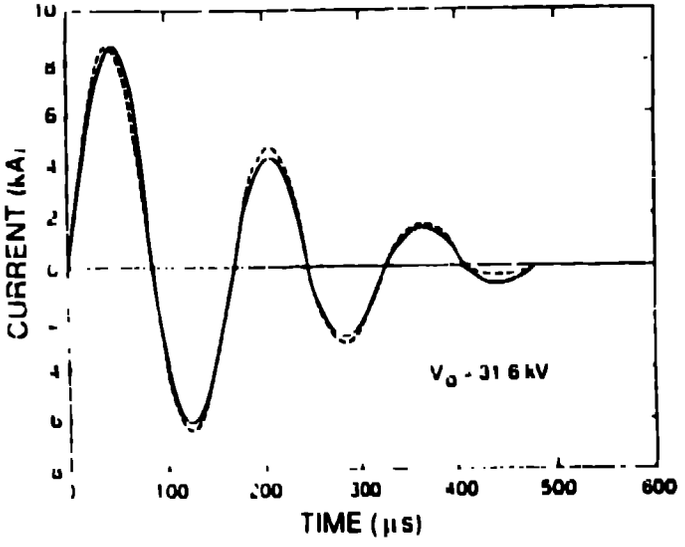

FIG. 4 The data taken at NRL is shown as a solid curve. The initial Marx-bank voltage was 31.6 kV. The dashed curve is the fit to the current evoluation predicted by our LCR theory using R = 0.3 Ω and V* = 1.8 kV.

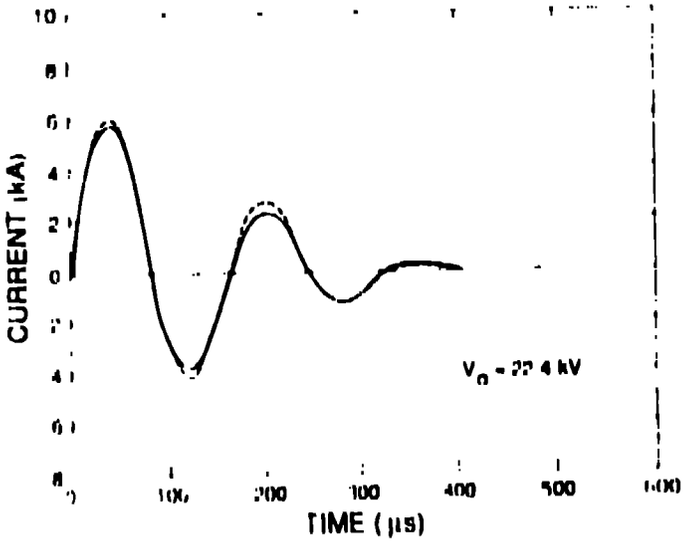

FIG. 5. With the same values of R and V* used in Fig. 4, but an initial Marx-bank voltage of 22.4 kV, the LCR theory predicts the current evolution shown by the dashed curve. The data taken by NRL is the solid curve.

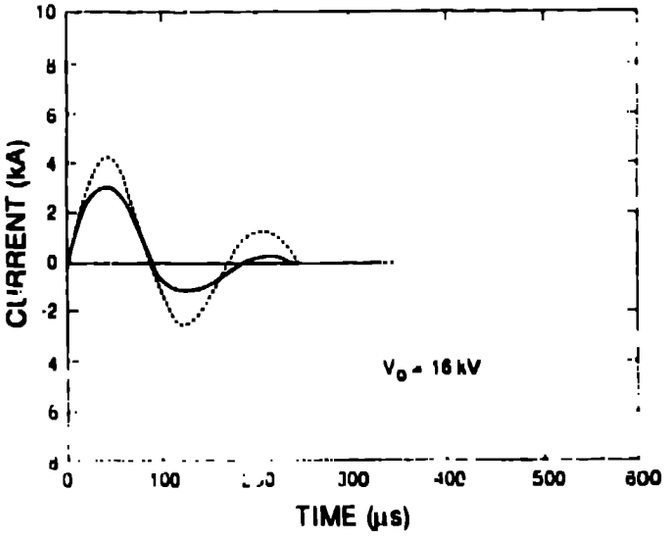

FIG. 6. With the same values of R and V* used in Fig. 4, but an initial Marx-bank voltage of 16.0 kV, the LCR theory predicts the current evolution shown by the dashed curve. The data taken by NRL is the solid curve.

With the external resistance, R, and the "medium" parameter, V*, determined, we then used these fixed values to predict the discharge at other starting voltages. Results are shown in Figs. (5) and (6). As shown, we again obtained excellent agreement in the mid-range of starting voltage. At the lowest voltage, agreement was not as satisfying. The correct number of oscillations prior to termination was obtained and the termination time was in agreement with the data, but amplitudes were not as good as for the other discharges. The experimental team that obtained the data expressed a belief that, in fact, the lowest voltage discharge was somewhat different from the others. The difference may be related to channel preparation.[10]

We then modeled, in the same way, an arc gap breakdown experiment performed at Texas Tech. The circuit inductance and capacitance were 226 nH and 1.9 μF, respectively. A publication by the team performing this experiment compared an arc resistance inferred from the data with that predicted by eight other theories. Only a theory by M. Kushner[12] fit the data reasonably well over the time history of the discharge. His theory yields an arc resistance that varies inversely with $I^{0.5}$. The other

theories fail badly after arc resistance achieves its minimum value. Our theory, using R = 1.0 Ω and V* = 0.92 kV, fits as well as Kushner's (see Figs. (7-9)). There is one critical difference between his scaling and ours. If one substitutes an $I^{-6/5}$ scaling in an LCR model, one finds that the arc resistive voltage drop, $R_a I$, becomes infinite at zero current. Therefore, no finite initial applied voltage is capable of starting a discharge current.

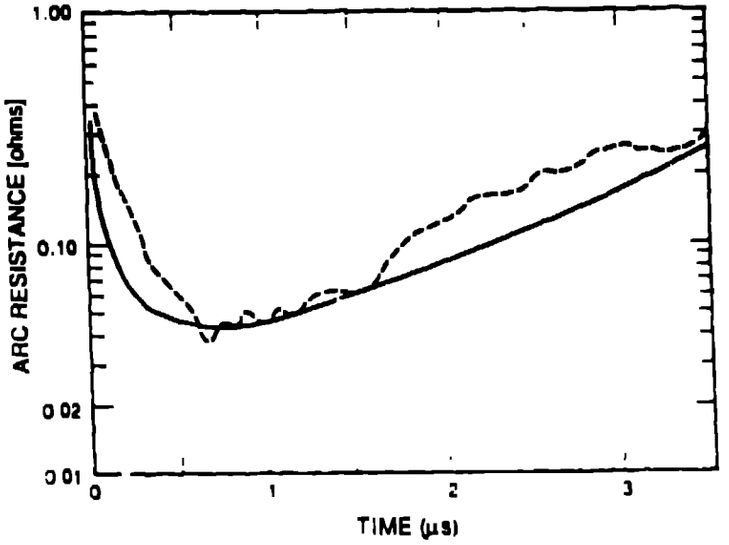

FIG. 7. The dashed curves in Figs. 7-9 are the same arc resistance *vs.* time plot inferred from discharge data. The solid curve is the arc resistance *vs.* time plot obtained by solving the LCR equations with R = 1.0 Ω and V* = 0.92 kV.

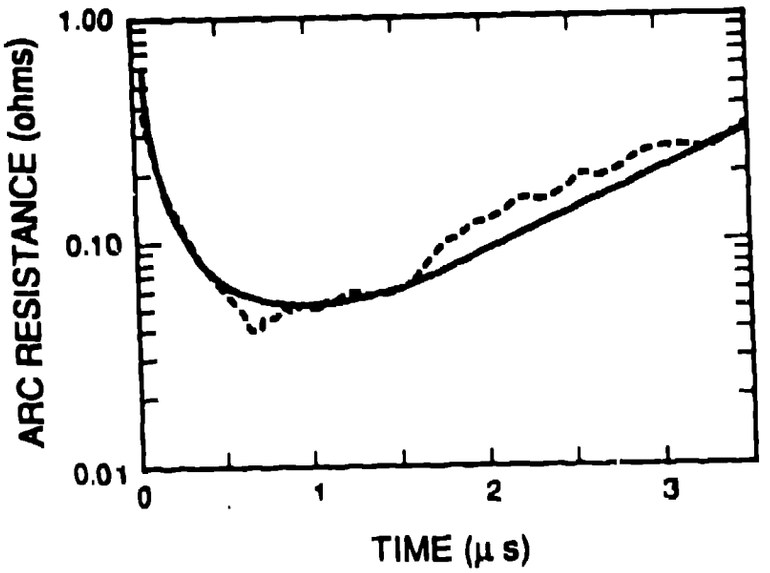

FIG. 8. The dashed curves in Figs. 7-9 are the same arc resistance *vs.* time plot inferred from discharge data. The solid curve is the arc resistance *vs.* time plot obtained from a theory by M. J. Kushner which predicts an inverse proportionality of arc resistance on current raised to the 6/5 power.

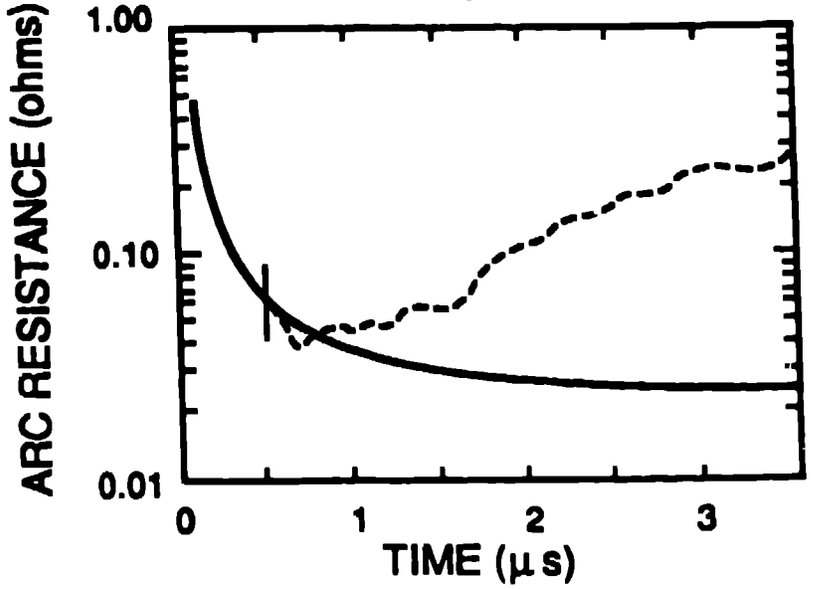

FIG. 9. The dashed curves in Figs. 7-9 are the same arc resistance *vs.* time plot inferred from discharge data. The solid curve is typical of plots of arc resistance *vs.* time using other theories of arc resistance as a function of current. Typically, those theories contain an inverse proportionality of arc current on time integrals of the current. Those integrals inhibit the increase of arc resistance after the discharge current peaks.

The only single scaling of arc resistance with current that allows both a finite threshold for current start and the possibility of abrupt current termination is R_a is proportional to $|I|^{-1}$ for small currents.

V. Summary

We have provided a brief overview of a generic macroscopic theory of electrical discharges. The generic theme is that there is a dissipative process (e.g., electrical resistivity) which, at small current, varies inversely with the magnitude of the current. This scaling of resistance with current is the only one which predicts both nonzero but finite field thresholds for the onset of discharge current and abrupt termination of current. The effects of self consistently produced and externally generated waves

on charge transport in current channels has been discussed and illustrated using simple examples. These effects include leaders. We have shown how the evolution of current channels is predicted by the theory. In particular, the theory may account for zigzagging and bifurcation of current channels.

Clearly, there is a need to understand the inverse scaling of resistivity with current magnitude at small current. Several ideas have been suggested. To date, none are supported by anything close to complete analysis. Research on this question is continuing..

Acknowledgement

The authors wish to thank D. J. Simons for his encouragement. This work was supported in part by a research grant from the U.S. Air Force Office of Scientific Research and an Institutionally-Support Research grant at the Los Alamos National Laboratory.

References

[1] R. T. Robiscoe, A. Kadish, and W. B. Maier II, "A Lumped Circuit Model for Transient Arc Discharges," *J. Appl. Phys.* 64(9), p. 4355, 1 Nov 1988.

[2] O. P. Judd and J. Y. Wada, "Investigations of a UV Preionized Electrical Discharge and a CO_2 Laser," *IEEE J. Quantum Electron.* **QE-10**, p. 12, 1974.

[3] W. B. Maier II, A. Kadish, and R. T. Robiscoe, "Comparison of the AWA Lumped-Circuit Model of Electrical Discharges with Empirical Data," *IEEE Trans Plasma Science* (in review).

[4] R. T. Robiscoe, W. B. Maier II, and A. Kadish, "Overdamped Arc Discharge Data and an AWA Model," (in preparation).

[5] A. Kadish, R. T. Robiscoe, and W. B. Maier II, "A Theory of Abrupt Termination and Spontaneous Restart of Electrical Current in Surface Flashover Arcs," *J Appl Phys* 66(4), p. 1579, 15 Aug 1989.

[6] A. Kadish, W. B. Maier II, and R. T. Robiscoe, "Theory of Electrical Discharges Initiated from a Large Charge Spot on Dielectric Surfaces," *J Appl Phys.* 66(9), p. 4123, 1 Nov. 1989.

[7] A. Kadish, W. B. Maier II, and R. T. Robiscoe, "A Theory of Weak Electrical Discahrges on Dielectric Surfaces," *J Appl Phys* 67(10), p. 6118, 15 May 1990.

[8] W. B. Maier II, A. Kadish, C. D. Sutherland, and R. T. Robiscoe, "A Distributed Parameter Wire Model for Transient Electrical Discharges," *J. Appl. Phys* **67**(12), p. 7228, 15 Jun 1990.

[9] R. E. Pechacek, D. P. Murphy, and R. A. Meger, "Characteristics of Laser-Guided Electric Discharges as a Function of Capacitor Bank Input Energy," Proceedings of the 1988 Annual Propagation Physics Review of the SDIO and DARPA of Army, Navy, and Air Force, 1988, pp. 225-228 (Naval Surface Warfare Center, Silver Spring, MD).

[10] R. E. Pechacek and D. P. Murphy, private communication,1990.

[11] T. E. Engel, A. L. Donaldson, and M. Kristiansen, "The Pulsed Discharge Arc Resistance and Its Functional Behavior," *IEEE Trans. Plasma Sci* **17**, p. 323, April 1989.

[12] M. J. Kushner, W. D. Kimura, and S. R. Byron, "Arc Resistance of Laser-Triggered Spark Gaps," *J. Appl Phys.* **58**(12), p. 1744, Sept. 1985.